IEEE Access
Multidisciplinary ⋮ Rapid Review ⋮ Open Access Journal

Received 12 January 2024, accepted 7 February 2024, date of publication 9 February 2024, date of current version 20 February 2024.

Digital Object Identifier 10.1109/ACCESS.2024.3364819

RESEARCH ARTICLE

Comparing Positioning Performance of LEO Mega-Constellations and GNSS in Urban Canyons

HARSHAL MORE, ERNESTINA CIANCA, (Member, IEEE), AND MAURO DE SANCTIS
Department of Electronics Engineering, University of Rome "Tor Vergata," 00133 Rome, Italy
Corresponding author: Harshal More (catchmemore@hotmail.com)

ABSTRACT The use of Low Earth Orbit (LEO) mega-constellations for Positioning, Navigation, and Timing (PNT) services has attracted a great deal of interest, as they could complement the Global Navigation Satellite System (GNSS) in specific conditions/environments. Despite the fact that it is recognized that the use of mega-constellations for positioning services could provide better performance in urban canyons, no work has provided an analysis of such performance improvement. This paper provides a statistical analysis of the performance in terms of availability and Geometric Dilution of Precision (GDOP) of the positioning service of some current mega-constellations in deep urban canyon environments and compares the performance with the one achieved by GNSS systems. A new geometric model for typical urban canyons is developed. The developed model has been used for the analysis of the availability and GDOP of the positioning service in two representative urban canyon areas, namely the city of London and the Manhattan district of New York City. The geometric parameters used in the simulations are derived by statistically processing publicly available data on the height and length of the buildings and the width of the streets in the considered urban areas.

INDEX TERMS Availability, GDOP, GNSS, LEO mega-constellation, positioning performance, urban canyon.

I. INTRODUCTION

The current landscape of mainstream Positioning, Navigation, and Timing (PNT) systems dominates the absolute market for large-scale PNT applications such as autonomous driving, timing and synchronization in telecommunications, power grid, network, financial transactions, scientific experiments, critical infrastructure operations such as energy supply networks, transport infrastructures, search and rescue operations, air traffic management, mapping and surveying, precision agriculture, unmanned aerial vehicle (UAV), etc. [1], [2], [3], and [4]. However, these applications face several threats due to the challenges and drawbacks of the mainstream Global Navigation Satellite Systems (GNSS) that can affect their performance and reliability. A major challenge is the vulnerability to signal degradation and interruptions caused by factors such as signal blockage or attenuation in urban environments, dense vegetation, or indoor environments. This can lead to reduced accuracy or even complete signal loss in certain situations. Furthermore, GNSS signals can be affected by atmospheric conditions, multipath interference, and satellite geometry, which can introduce errors in positioning and timing. Furthermore, GNSS signals are susceptible to deliberate interference or jamming, which can disrupt their availability and integrity [1], [2], [4].

These challenges highlight the need for alternative solutions and technologies to enhance the performance and robustness of GNSS in challenging environments. However, the use of Low Earth Orbit (LEO) constellations for PNT has attracted more and more interest due to the thousands of satellites launched or planned to be launched by private companies such as Starlink, OneWeb and Kuiper for applications such as the global internet, IoTs, telecommunications, etc. [5].

LEO satellites offer several advantages in terms of cost-effectiveness, availability, positioning accuracy, and

The associate editor coordinating the review of this manuscript and approving it for publication was Ze Ji.

robustness in challenging environments. Moreover, the faster orbital velocity of LEO satellites compared to Medium Earth Orbit (MEO) GNSS satellites enables effective Doppler-based positioning techniques [6]. Faster movement also mitigates multipath effects in urban canyons, as reflections are not static over shorter time intervals [7]. Furthermore, LEO mega-constellations boast increased satellite visibility and lower signal attenuation with the availability of Ka/Ku frequency bands further enhancing robustness in GNSS-denied scenarios where stronger signals are crucial [8].

The urban canyon environment is characterized by dense tall buildings and narrow streets, which create unique challenges to satellite navigation and communication systems. The presence of tall buildings in urban canyons causes GNSS signals to often result in non-line-of-sight (NLOS) conditions, where the direct line-of-sight (LOS) between the GNSS receiver and the satellite is obstructed. These signals are reflected off buildings, resulting in distorted and delayed low-power signals.

Although researchers and industry players are actively exploring and developing techniques to leverage the advantages of LEO constellations for PNT, no work has analyzed the performance of the LEO mega-constellations navigation system in a deep urban canyon environment. The performance of GNSS systems in urban canyon scenarios has been extensively studied but mainly experimentally in specific locations. Some works have also simulated the performance of GNSS systems in urban canyons by using 3D city models or city street models on Geographic Information Systems (GIS) [9], [10], [11], [12], [13], [14], [15], [16], [17], [18], [19], [20], [21], [22], [23], [24], [25], [26], [27]. The detailed literature review of these works is discussed in Section II-B. Nevertheless, these models have not been applied to LEO mega-constellations. Moreover, those models are not easily extendable to other locations as 3D models and GIS data are not widely available.

This paper proposes a new geometric model for urban canyons. The developed model has been used to compare the performance of the positioning service in terms of availability and Geometric Dilution of Precision (GDOP) of two well-known LEO mega-constellations (Starlink and OneWeb) and traditional GNSS systems (GPS and Galileo) in two representative urban canyons environments, namely the city London and the Manhattan district of New York City. The simulations are based on geometric parameters that are derived by statistically processing publicly available data about the height and length of the buildings and the width of the streets in those areas. However, the model could also be used for performance analysis in other cities/areas or in the design phase of a dedicated constellation for positioning.

The paper is organized as follows: Section II provides a review of the literature on the current state of the art in LEO-PNT and the proposed approaches/models to analyze the performance of GNSS in urban canyon environments. In Section III, comprehensive mathematical modeling is presented for the urban canyon model, satellite visibility estimation in urban canyons, street direction within the canyons, statistical analysis of input parameters of urban canyon dimensions, and definition of GDOP. Section IV presents a detailed performance comparison, statistical analysis, and results. Finally, conclusions are drawn in Section V.

II. LITERATURE REVIEW

The review of the literature is divided into two subsections. The first part highlights the state-of-the-art LEO infrastructure for PNT solutions, while the second part gives an overview of the proposed approaches/models used to analyze the GNSS performance in urban canyon environments.

A. STATE-OF-THE-ART IN LEO-PNT INFRASTRUCTURE

Recently, various approaches to the implementation of LEO-PNT have been proposed. Each of these approaches has its advantages and disadvantages highlighted as follows:

- Dedicated LEO-PNT: In the dedicated LEO-PNT approach, an independent LEO constellation is designed to deliver PNT services. Nevertheless, the development and deployment of such standalone infrastructure is expensive. Several studies have explored this area. Different LEO navigation constellation configurations have been proposed which are optimized to enhance the performance in terms of GDOP and availability [28]. In the article [29], hybrid LEO constellations are designed for broadband Internet access that can be used for augmented navigation purposes with global coverage and at most three visible satellites. In the paper [6], a constellation of 264 satellites at 800 Km polar orbit is proposed, which can be used for Doppler-based PNT. Paper [30] shows the optimization of the MEO constellation for global coverage and the hybrid LEO/GSO constellation to provide a navigation service over Europe. Moreover, private sectors such as Xona Space Systems are planning to launch 300 satellites in LEO for next-generation GNSS [31].
- LEO-PNT with Hosted payload: In this case, additional navigational instruments or systems to provide the PNT service are hosted by the main payload. This solution is cheaper than the dedicated LEO-PNT, but the complexity of the subsystem design is higher. Moreover, this approach has some security issues. In the paper [32], authors have evaluated pseudorange and carrier phase measurements from the Luojia-1A remote sensing satellite. In March 2017, the European GNSS Agency (GSA) selected Eutelsat Communications to develop, integrate, and operate its next-generation EGNOS payload, to be hosted on the EUTELSAT 5 West B satellite [33]. Overall, this approach is good for experimental stages.
- Fused LEO-PNT: Recently, this new approach has been proposed where the onboard hardware is not modified but the navigation information is inserted in the communication/remote sensing signal trying to minimize the impact on the primary purpose of that signal. The main problem with this approach is the need

to implement complicated scheduling of the downlink beams as the navigation system needs to have at least 4 satellites in visibility, which is not required in communication systems. This requires assistance from the satellite operator for additional steering and transmission costs [34].

- LEO-PNT through Signal of Opportunity (SoO): In this case, the navigation system uses signals that are transmitted by LEO satellites for other purposes (communication or remote sensing). Most of the works on the use of SoO focus on the use of signals transmitted by already deployed LEO mega-constellations, such as OneWeb, Starlink, and Orbcomm [35], [36], [37]. In this case, many visible satellites are available at a given epoch and there is no need for an independent infrastructure or modified hardware onboard. However, the design of the receiver, which must be capable of extracting Time-of-Arrival (TOA) measurements from signals not intended for navigation and sometimes with unknown structure, is much more complex. Moreover, there is the problem of getting the satellite ephemerides that are not transmitted by the LEO satellite as they were originally born for communication purposes. Using the information that can be found in the Two-Line-Element (TLE) files which are tracked and publicly published on a daily basis by the North American Aerospace Defence Command (NORAD) [38], introduces an error of a kilometers due to several sources of perturbations [39]. Additionally, tight synchronization is not feasible as such LEO satellites for communication purposes typically lack atomic clocks. However, this approach has significant appeal for satellite operators who can avoid investing in an expensive new space infrastructure.

In general, considering the possibility of using already deployed infrastructures for other services (communication, internet, telephone, etc.) goes in the direction of more sustainable use of the space which is one of the main current challenges [8], therefore this paper focuses on investigating the latter approach.

B. PROPOSED APPROACHES/MODELS FOR GNSS PERFORMANCE IN URBAN CANYON

Various approaches have been proposed for performance in urban canyon models based on their intended applications such as communication, navigation, urban climate research, etc. A review of the literature [9], reveals different methods used to estimate the Sky View Factor (SVF), including geometric methods, fish-eye photographic methods, Global Positioning System (GPS) methods, simulation methods utilizing 3D city models or Digital Surface Models (DSM), and big data approaches employing street view images. Each method has its advantages and disadvantages depending on the specific application.

In the article [10], the author introduces modified propagation models tailored for urban canyons, which require knowledge of satellite signal properties to estimate path losses within the canyons. Another approach involves the use of the City Geography Markup Language (CityGML) model to represent urban environments, which is subsequently converted into a STereoLithography (STL) surface model [11]. DLR has developed software that provides a comprehensive overview of model parameters accessible to users of the Land Mobile Satellite Channel Model (LMSCM) and describes its effects within the artificial scenery of LMSCM, where urban canyon parameters are modeled as Gaussian distributions [12].

Several urban canyon models have been used for investigating the multipath in GNSS systems. The article [13], is focused on using large Virtual Reality City Models (VRCM) to accurately determine the local environment and code multipath. For the simulations, a street in London has been considered. An important issue of large VRCM is that it requires extensive data acquisition, including high-resolution imagery, terrain data, and 3D building models. In the paper [14], authors use a 3D DSM to improve positioning accuracy by capturing intricate details of the urban environment. However, the DSM is constructed using high-resolution data, including aerial imagery and LiDAR. Paper [40], demonstrates the tight integration of constructive utilization of NLOS GNSS signals and a 3D city model. Furthermore, the authors have addressed the issue of data acquisition and processing, model accuracy, and computational requirements for this tight integration process.

Some research focuses on leveraging the shadow matching cast by urban structures to improve the positioning accuracy of the GNSS. In the paper [15], the authors describe the algorithm for a 3D city model using shadow matching. Some related works on similar techniques can be found in [16] and [17]. However, shadow matching has potential limitations or constraints such as dependence on lighting conditions or dynamic urban environments. GNSS performance has been evaluated in specific regions and cities, such as London, where experimental results have been tested using a Virtual Reality Modeling Language (VRML) urban model of central London to analyze the visibility and availability of the GNSS system and the impact of building height, street width, and signal blockage on positioning accuracy [18], [19], [20], [21].

The performance of Precise Point Positioning (PPP) techniques for surveying applications in some urban areas of Turkey, using GPS and GPS+GLONASS observations is examined by the authors in research work [41]. Similar work has been conducted in [24] and [25], Seoul [26] and Hong Kong [27]. Some studies have investigated integration strategies for performance improvement in urban canyons. For instance, in the article [22], a loosely coupled integration approach has been proposed, which combines GNSS receiver and Doppler sensor measurements using a graph optimization framework for positioning in urban canyons, specifically in the city of New York.

Research [42] explores the efficacy of single-frequency GPS-Galileo systems for attitude determination in environments with limited satellite availability with experimental

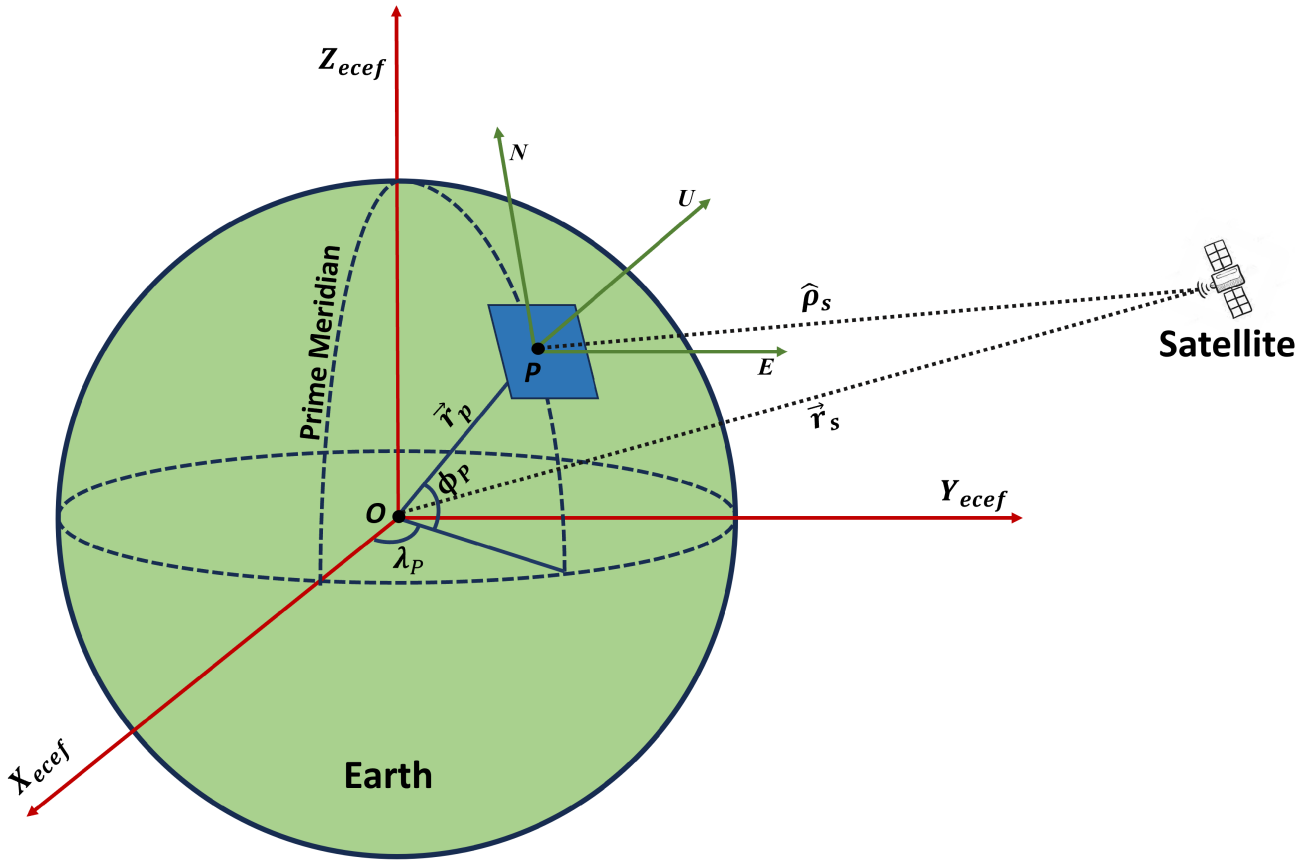

FIGURE 1. Reference frames ECEF (X_{ecef}, Y_{ecef}, Z_{ecef}) and ENU (E, N, U) of user located at geocentric P ($\vec{r}_p$, λ_p, ϕ_p). Satellite position vectors $\hat{\rho}_s$ and $\vec{r}_s$ are measured from the user and the center of the Earth O respectively.

setup and data analysis. In the paper [23], authors have demonstrated the effectiveness of the multi-UAS cooperation framework and the improved navigation accuracy achieved considering the generalized dilution of precision in Manhattan. Authors in the paper [43] propose a building update monitoring algorithm based on sky visibility estimation using GNSS and LEO satellites. In addition, the potential of mega-constellation-augmented GNSS for fault-free high-integrity positioning in both open-sky and urban areas of Tucson, Arizona is evaluated in the article [44].

However, existing literature primarily concentrates on assessing the performance of mainstream GNSS systems or GNSS systems aided with other navigation systems. Numerous methodologies have been employed to model or simulate urban canyons. This paper introduces a new geometric approach to statistically model urban canyons and to evaluate the performance of LEO mega-constellations in comparison to conventional GNSS systems.

III. MATHEMATICAL MODELING

This Section presents the mathematical modeling of satellite visibility from the user in an urban canyon as a function of urban canyon geometry. Realistic geometric parameters are extracted from the statistical analysis of publicly available data for two representative urban canyon areas. The geometric model is then used in simulation analysis for the positioning performance evaluation in terms of two of the most important metrics, i.e. service availability (visibility of at least 4 satellites) and GDOP (effect of visible satellite geometry on position estimation accuracy). Table 1 lists the description of all symbols and letters used in this paper.

A. DEFINITION OF FRAME OF REFERENCE

Initially, the reference frames are defined as shown in Fig. 1. Earth-Centered-Earth-Fixed (ECEF) reference system is represented by X_{ecef}, Y_{ecef}, Z_{ecef} axes with the origin located at the center of the Earth O. The user is located at P with a local reference frame defined by the East-North-Up (ENU) coordinate system. The ENU reference system is transformed into ECEF by two rotations along the geocentric latitude (λ_p) and longitude (ϕ_p). Therefore, the rotation matrix, R is given by Eq. (1), [45]:

$$R = \begin{pmatrix} -\sin\lambda_p & -\cos\lambda_p \sin\phi_p & \cos\lambda_p \cos\phi_p \\ \cos\lambda_p & -\sin\lambda_p \sin\phi_p & \sin\lambda_p \cos\phi_p \\ 0 & \cos\phi_p & \sin\phi_p \end{pmatrix} \quad (1)$$

From Fig. 1, the LOS unit vector, $\hat{\rho}_s$ from the user to the satellite is given by Eq. (2):

$$\hat{\rho}_s = \frac{\vec{r}_s - \vec{r}_p}{||\vec{r}_s - \vec{r}_p||} \quad (2)$$

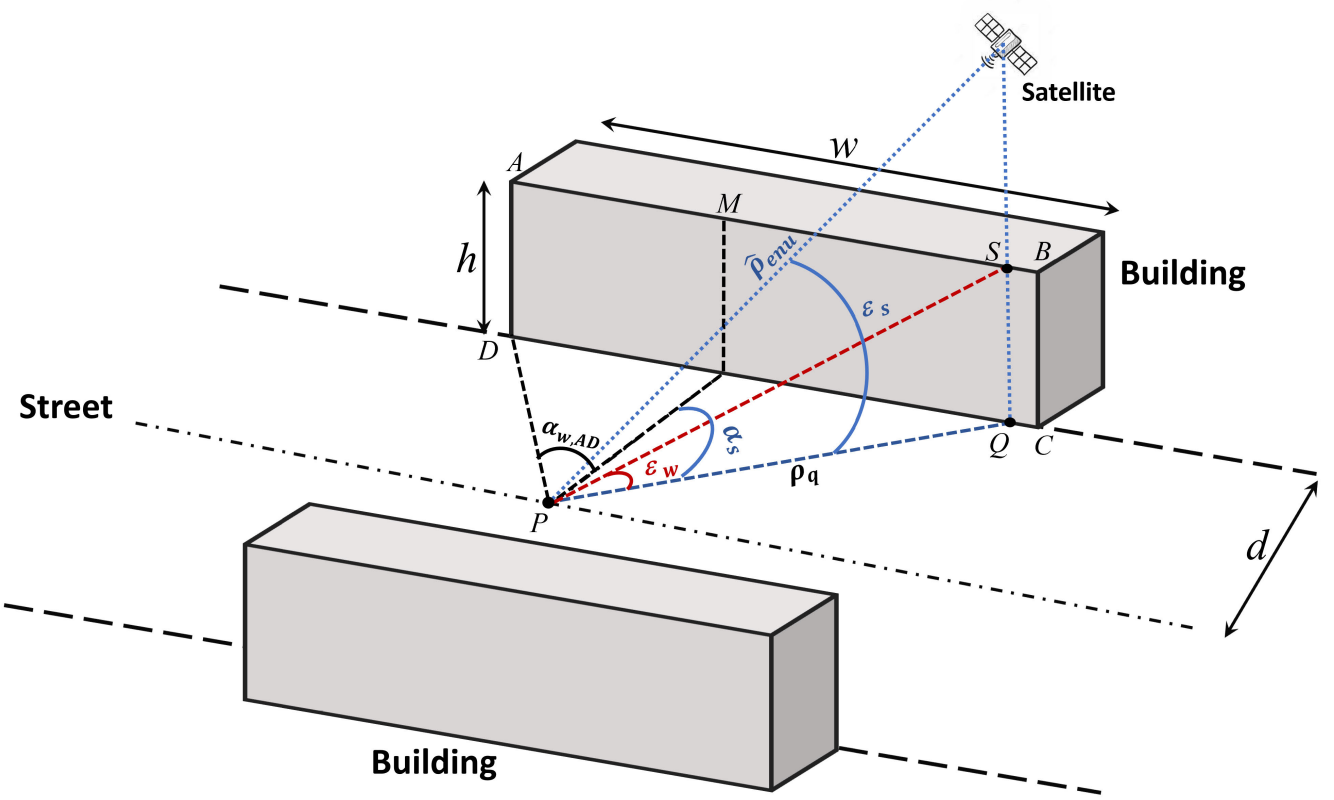

FIGURE 2. Urban canyon geometry defined using parameters *h*, *w*, *d* and satellite position with respect to a user located at P. *h*, *w*, and *d* are obtained using statistical processing of raw data.

where $\vec{r}_s = [X_s, Y_s, Z_s]$ and $\vec{r}_p = [X_p, Y_p, Z_p]$ are the position of the satellite and user in ECEF frame, respectively.

B. SATELLITE VISIBILITY AS A FUNCTION OF URBAN CANYON GEOMETRY

In GNSS, the user position is estimated using at least four TOA measurements from direct LOS satellites at a given epoch. In urban canyon environments, direct LOS might be blocked due to the varying dimensions of the buildings. In this Section, we have used a geometric approach to develop a model that connects the satellite visibility to the main characteristics of the urban canyons (height and length of buildings, width and orientation of the streets).

Fig. 2 shows the geometry of the finite-length urban canyon and the position of the satellite with respect to the user at P. ABCD is the wall of the building that has width w and height h. d is half the width of the street. These three input parameters are obtained after statistical analysis of the available database as explained in Section III-D. S and Q are points at an instant when the satellite is passing over the urban canyon. This dimension of the building is defined in the local ENU with respect to the P explained in Section III-C.

The Visibility of the satellite from P is calculated using the elevation angle (ϵ_s), and the azimuth angle (α_s). Using trigonometry, ϵ_s and α_s from P to the satellite are calculated using Eq. (3) and Eq. (4):

$$\epsilon_s = \arcsin(\hat{\rho}_{enu}.\hat{u}) \tag{3}$$

$$\alpha_s = \arctan\left(\frac{\hat{\rho}_{enu}.\hat{e}}{\hat{\rho}_{enu}.\hat{n}}\right) \tag{4}$$

where $\hat{\rho}_{enu} = [R^T].\hat{\rho}_s$ and $\hat{e}$, $\hat{n}$, $\hat{u}$, are unit position vectors from the user. Similarly, at building edges BC and AD, the azimuth angles are presented by $\alpha_{w,BC}$ and $\alpha_{w,AD}$ respectively, which are estimated using Eq. (5):

$$\alpha_{w,BC} = \alpha_{w,AD} = \arccos\left(\frac{d}{\rho_c}\right) \tag{5}$$

where ρ_c is a distance measured from P to C (see Fig. 3 and Fig. 2). Therefore, when the satellite passes over the urban canyon, the elevation angle from the user to the building edges (ϵ_w) is defined by Eq. (6):

$$\epsilon_w = \begin{cases} \arctan\left(\frac{h}{\rho_q}\right), & \text{if } \alpha_s \in [\alpha_{w,AD}, \alpha_{w,BC}], \\ \epsilon_{min}, & \text{otherwise.} \end{cases} \tag{6}$$

where ϵ_{min} is the minimum elevation mask angle without the urban canyon and ρ_q is a distance measured from P to Q (as shown in Fig. 3) is estimated by Eq. 7:

$$\rho_q = \frac{d}{cos(\alpha_s)} \tag{7}$$

TABLE 1. Symbols and letters description.

Symbol	Description
$\vec{A}_{ECEF}$	ECEF vector of the building point A
$\vec{A}_{ENU}$	ENU vector of the building point A
α_s	Azimuth angle of the satellite from user
$\alpha_{w,AD}$	Azimuth angle of the building edge AD from the user
$\alpha_{w,BC}$	Azimuth angle of the building edge BC from the user
$\vec{B}_{ECEF}$	ECEF vector of the building point B
$\vec{B}_{ENU}$	ENU vector of the building point B
β	Angle from user to point B
b_w	Bandwidth of Kernel density estimator
c	Weibull scale parameter
d	Half street width of the urban canyon
e	Satellite orbit eccentricity
ϵ_{min}	Minimum elevation mask angle
ϵ_s	Elevation angle of the satellite from the user
ϵ_w	Elevation angle of the building top edge from the user
γ	Angular direction of urban canyon
h	Urban canyon building height
H	Linearized measurement matrix
K	Kernel function
k	Weibull PDF shape parameter
λ_p	User geocentric longitude
μ_{gdop}	Mean GDOP of sample user IDs
$\vec{M}_{ECEF}$	ECEF vector of the building point M
$\vec{M}_{ENU}$	ENU vector of the building point M
n	Total number of data samples
ϕ_p	User geocentric latitude
R	Rotation matrix ENU to ECEF
$\vec{r}_p$	User position vector in ECEF
$\vec{r}_s$	Satellite position vector in ECEF
$\hat{\rho}_{enu}$	Unit position vector of satellite in ENU
$\hat{\rho}_s$	Unit position vector of satellite in ECEF
ρ_c	Distance between user and building point C
ρ_q	Distance between user and building point Q
$\hat{\sigma_d}$	Standard deviation of data samples
w	Urban canyon building width

In this way, the satellite visibility from the user at P is estimated as:

$$\epsilon_s \geq \epsilon_w \tag{8}$$

C. THE DIRECTION OF URBAN CANYON STREET

The direction of the canyon street with respect to the direction of the satellite motion also affects visibility [46]. To analyze this, the canyon is rotated by the angle γ as shown in Fig. 3. The ENU coordinates of the points of the building B, M, and A (see Fig. 2 and 3) are defined using Eq. (9):

$$\begin{cases} B_E = \rho_c \cos(\beta + \gamma), \\ B_N = \rho_c \sin(\beta + \gamma), \\ B_U = h \\ \\ M_E = d \cos(\gamma + \pi/2), \\ M_N = d \sin(\gamma + \pi/2), \\ M_U = h, \\ \\ A_E = \rho_c \cos(\gamma - \beta + \pi), \\ A_N = \rho_c \sin(\gamma - \beta + \pi), \\ A_U = h, \end{cases} \tag{9}$$

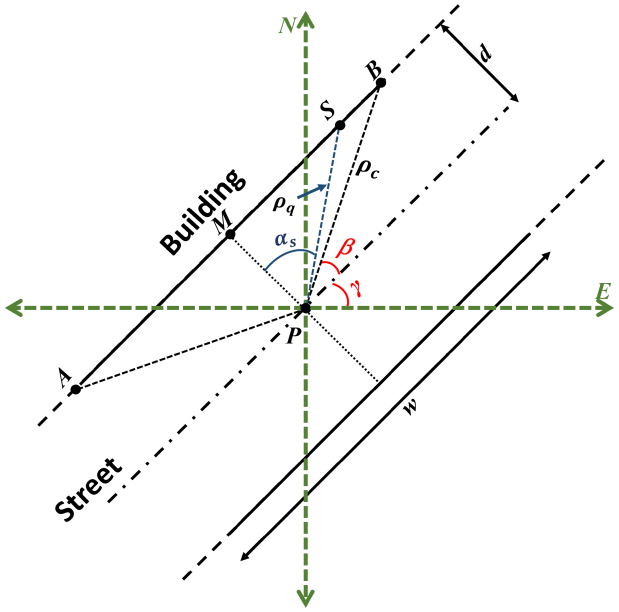

FIGURE 3. Direction of the urban canyon (top view) which rotated by an angle γ from $-\pi$ to π with respect to ENU. Points *A*, *S*, *B* are projected over points *D*, *Q*, *C* (as shown in Fig. 2) respectively.

where, ρ_c is maximum distance of ρ_q at C with $\forall\gamma \in [-\pi, \pi]$, and:

$$\beta = \arctan\left(\frac{d}{w/2}\right) \tag{10}$$

Further, ENU coordinates of the building point are transformed in the ECEF system using matrix R as shown in Eq. 11:

$$\begin{cases} \vec{B}_{ENU} = [B_E, B_N, B_U] \\ \vec{B}_{ECEF} = [R].\vec{B}_{ENU} \\ \\ \vec{M}_{ENU} = [M_E, M_N, M_U] \\ \vec{M}_{ECEF} = [R].\vec{M}_{ENU} \\ \\ \vec{A}_{ENU} = [A_E, A_N, A_U] \\ \vec{A}_{ECEF} = [R].\vec{A}_{ENU} \end{cases} \tag{11}$$

D. STATISTICAL ANALYSIS OF INPUT PARAMETERS FOR URBAN CANYON DIMENSIONS

Once the urban canyon model is developed, the simulation is tested for a user located in two locations characterized by urban canyons with different characteristics. Input parameters h, d, w, and γ are needed to define the geometry of the urban canyon. However, it is important to note that input parameters may not always be publicly available or accurate, so it is essential to carefully consider the quality and reliability of the data by statistical analysis. Once a data set is available, statistical analysis is performed using descriptive statistics by calculating mean, median, standard deviation, range, and

outliers. Then the kernel density estimator (KDE) is used to estimate the probability density function (PDF) for these parameters. KDE for $x_1, x_2, \ldots, x_n$ samples of corresponding input parameters given by Eq. (12), [47]:

$$\hat{f}(x) = \frac{1}{nb_w} \sum_{i=1}^{n} K\left(\frac{x - x_i}{b_w}\right) \tag{12}$$

where n is the total number of samples. K is the kernel (non-negative function), b_w is a KDE bandwidth parameter, which is obtained using Scott's rule of thumb [48]:

$$b_w \approx 1.06\hat{\sigma_d}.n^{-1/5} \tag{13}$$

$\hat{\sigma_d}$ is the standard deviation of data samples. The obtained PDF is used in the Curve Fitting Toolbox (CFT) in Matlab to find the best fitting distribution [49]. Different distribution models [50] have been tested among which the Weibull PDF is found to be the best fit for both cities. The Weibull PDF distribution is given as Eq. (14):

$$\hat{f}(x) = \frac{k}{c}\left(\frac{x}{c}\right)^{k-1} \exp\left(-\left(\frac{x}{c}\right)^{k}\right) \tag{14}$$

where $\hat{f}(x) \geq 0, x \geq 0, k > 0, c > 0$, k is the shape and c is the scale parameter for the Weibull curve.

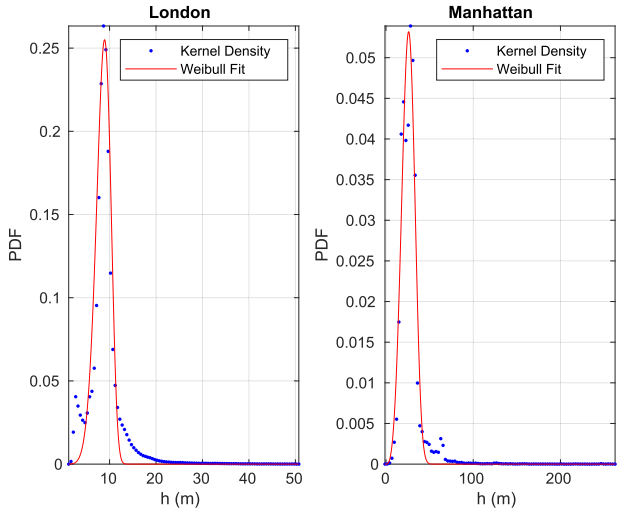

FIGURE 4. Weibull PDF and KDE of the building height (h). In both urban canyon areas, the probability of taller buildings is low with respect to h of all the buildings across the entire city.

Analyzing the depth of the urban canyons in the Manhattan district of New York City and London requires a data set that includes information on the heights of all buildings. The height data set used for this paper is [51] and [52] for London and Manhattan respectively. Fig. 4 shows the Weibull PDF and KDE curve of building height h. From the PDF is evident that in London most of the buildings have heights of around 15 m while in Manhattan they have higher heights, which are around 30 m. It is well known that for instance in Manhattan there are much taller buildings, with heights

TABLE 2. Goodness of fit parameters for height (h) achieved with Weibull PDF.

Parameters	Value for London (m)	Value for Manhattan (m)
k	9.173	28.02
c	6.275	3.908
SSE	0.02158	0.0006242
R-square	0.914	0.9509
Adjusted R-square	0.9132	0.9504
RMSE	0.01484	0.002524

from 200 to 500 m. However, these represent a very small percentage and are in the tail of the PDF. Table 2 shows the goodness of fit for h. Parameters c and k are estimated with confidence bounds of 95%.

The urban canyon's street width (2d) data is sourced from OpenStreetMap (OSM) [53] and is subjected to a processing method similar to h. The Weibull PDF is found to be the best fit as shown in Fig. 5. The detailed goodness of fit for $2d$ is highlighted in Table 3. c and k are estimated with confidence bounds of 95%.

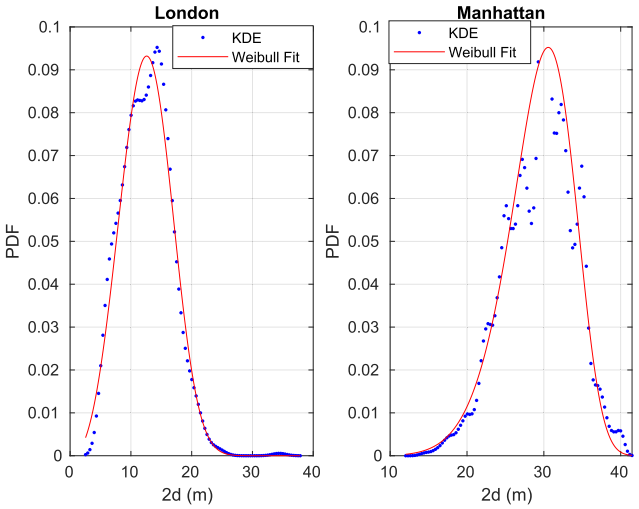

FIGURE 5. Weibull PDF and KDE of the street width $2d$.

TABLE 3. Goodness of fit parameters for street width ($2d$) achieved with Weibull PDF.

Parameters	Value for London (m)	Value for Manhattan (m)
k	14.0175	31.3004
c	3.5348	0.4928
SSE	0.0018	0.0166
R-square	0.9841	0.8684
Adjusted R-square	0.9839	0.8671
RMSE	0.0043	0.0130

Parameter w in London is generated using an exponential distribution with an average of 42 m and a median of 34 m [55]. For Manhattan, a similar distribution for w is

TABLE 4. Orbital configurations of mainstream GNSS (GPS, Galileo) and LEO mega-constellations (Starlink, OneWeb) [54]. The table shows the total number of planned satellites for mega-constellations.

Constellation	Application	Altitude of orbit (Km)	Mean Velocity (Km/s)	Period (min)	Planes per Orbit	Satellites per Plane	Total Number of Sat	Inclination (Deg)	e	Frequency Bands Downlink
GPS	Navigation	20200	3.88	720	6	4	24	55	0	L1: 1575.42 Mhz L2: 1227.60 MHz
Galileo	Navigation	23222	3.66	845	3	8	24+6	56	0	E: 1176-1207 MHz
Starlink	Global Internet Broadband	335.9 340.8 345.6 550 1110 1130 1275 1325	7.5576 7.5839 7.6098 7.4984 7.2139 7.2696 7.2128 7.1679	91-112	9 7 9 24 32 8 5 6	277 354 283 66 50 50 75 75	11943	42 48 53 53 53.8 74 81 70	0	K-band: 17.8-18-5 GHz 18.8-19.3 GHz 19.7-20.2 GHz V-band: 37.5-42.0 GHz
OneWeb	Global Internet Broadband	1200	7.24	110	18	36	648	87.9	0	Ka/Ku Bands: 17.8-18.6 GHz 18.8-19.3 GHz

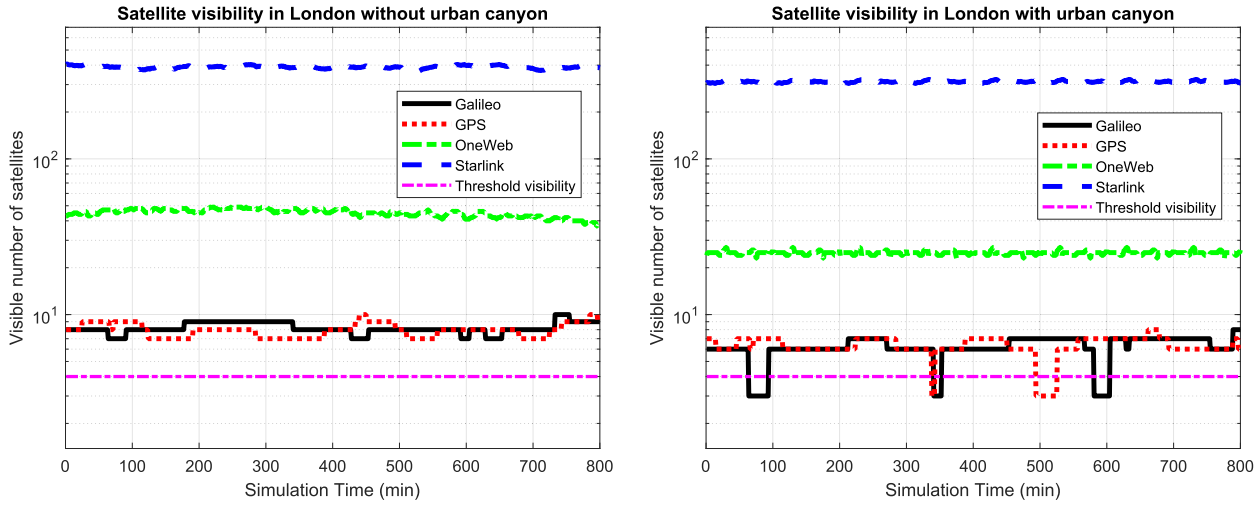

(a) London without urban canyon

(b) London with urban canyon

FIGURE 6. Visibility of constellations in London for a sample user ID over a simulation time of 800 minutes.

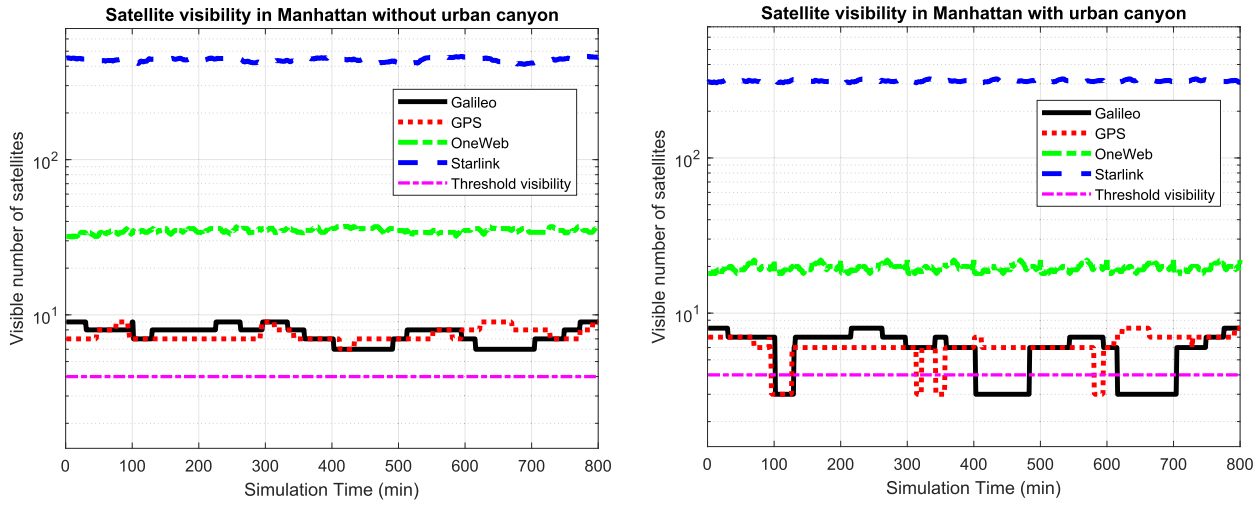

(a) Manhattan without urban canyon

(b) Manhattan with urban canyon

FIGURE 7. Visibility of constellations in Manhattan for a sample user ID over a simulation time of 800 minutes.

assumed. The orientation of the urban canyon is determined by γ, which is derived from a uniform distribution ranging from $-\pi$ to π.

In this way, this analysis can provide insight into the statistical distribution dimensions of urban canyons in both cities and help to obtain realistic input parameters

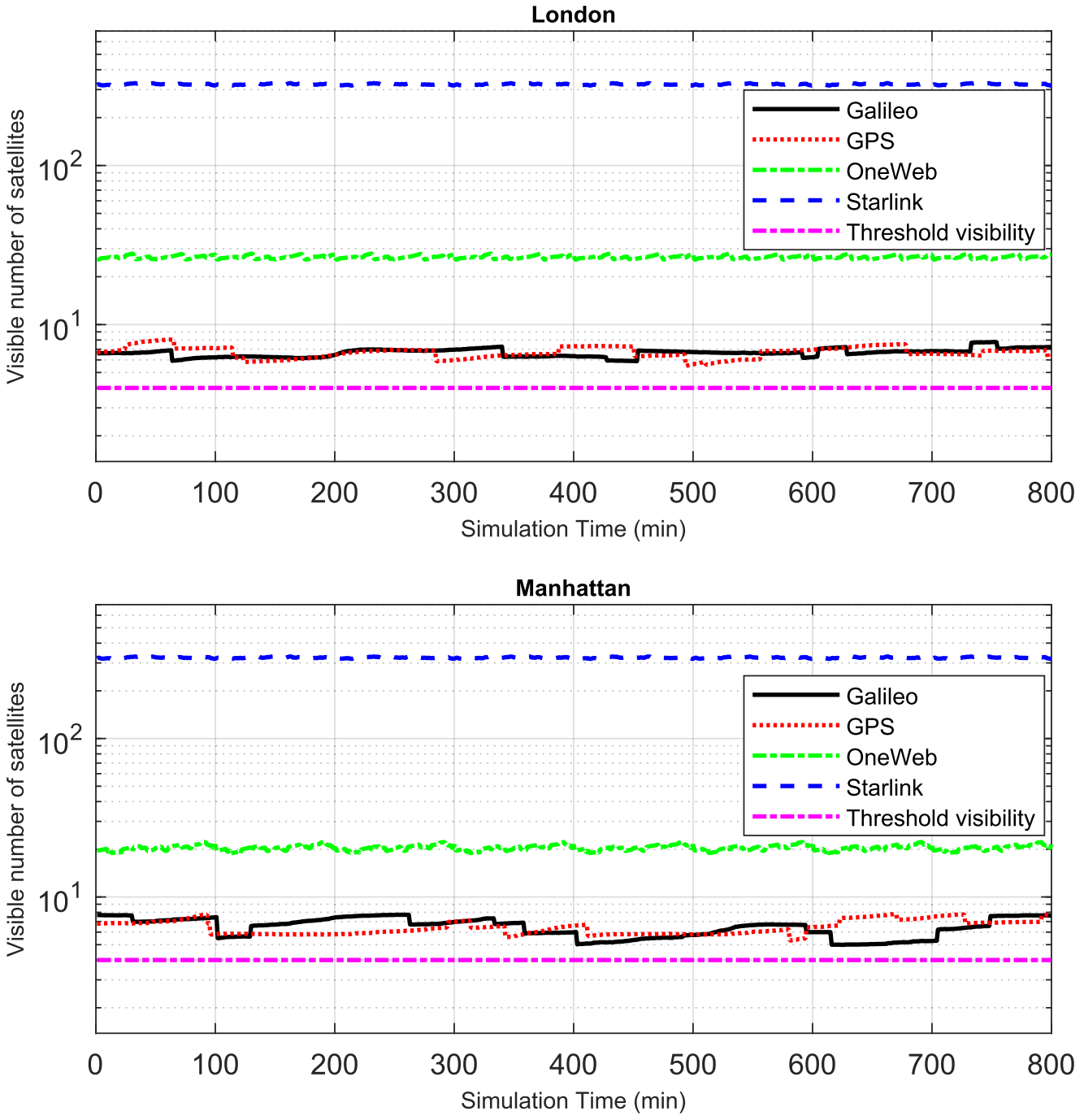

FIGURE 8. Mean satellite visibility of 100 sample user IDs over a simulation time of 800 minutes with the urban canyon in London and Manhattan.

for the simulation with the help of the obtained distribution.

E. GDOP

In navigation, the accuracy of user positioning depends on the geometric configuration of the satellite, i.e. Dilution of Precision (DOP). TOA measurements are imported from all visible satellites to estimate the DOP [37]. Matrix GDOP is estimated using the DOP. To calculate the DOP, the matrix H is defined using the partial differentiation of the residuals of the TOA measurements with respect to the user position and time:

$$H = \begin{pmatrix} h_{x1} & h_{y1} & h_{z1} & 1 \\ h_{x2} & h_{y2} & h_{z2} & 1 \\ \cdot & \cdot & \cdot & \cdot \\ \cdot & \cdot & \cdot & \cdot \\ \cdot & \cdot & \cdot & \cdot \\ h_{xj} & h_{yj} & h_{zj} & 1 \end{pmatrix} \tag{15}$$

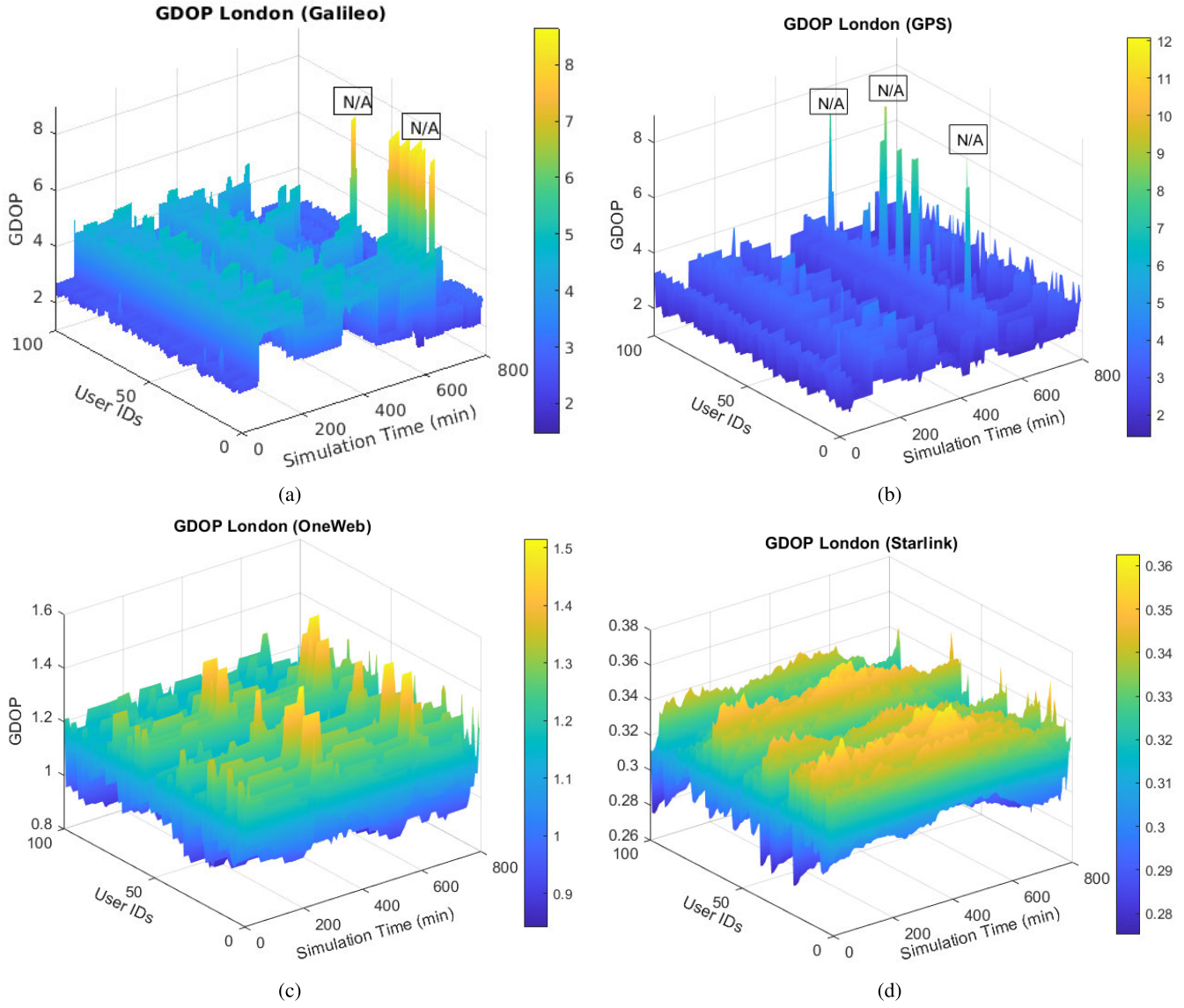

FIGURE 9. GDOP variation for 100 sample user IDs in London for Galileo, GPS, OneWeb, Starlink over a simulation time of 800 minutes. In Fig. 9a and Fig. 9b, N/A is the unavailability of a sufficient number of visible satellites for a certain sample user ID at a given epoch. Note the color bars to interpret the scales of the respective graphs.

where $h_{xj} = \frac{X_{sj}-\hat{X}_p}{||\rho_{sj}||}$, $h_{yj} = \frac{Y_{sj}-\hat{Y}_p}{||\rho_{sj}||}$, $h_{yj} = \frac{Z_{sj}-\hat{X}_p}{||\rho_{sj}||}$ are linearized unit vectors of j_{th} visible satellites, considering that:

$$||\rho_{sj}|| = \sqrt{(X_{sj} - \hat{X}_p)^2 + (Y_{sj} - \hat{Y}_p)^2 + (Z_{sj} - \hat{Z}_p)^2} \tag{16}$$

where $[\hat{X}_p, \hat{Y}_p, \hat{Z}_p]$ is the estimated user position. The overall matrix DOP can be obtained as:

$$DOP = (H^T H)^{-1} \tag{17}$$

Finally, in accordance with our interest, GDOP is defined as:

$$GDOP = \sqrt{trace(DOP)} \tag{18}$$

This evenness in satellite geometry (GDOP) is important to improve accuracy. Table 5 shows that the ideal GDOP is less than 1. The excellent values of GDOP are in the range of 1-2, and the good ones are in the range of 2-5. Mainstream GNSS has an average excellent GDOP for a ϵ_{min} of 5°, [56]. In this article, the GDOP remains undefined in scenarios where a sufficient number of visible satellites are not available (N/A).

IV. PERFORMANCE COMPARISON ANALYSIS

Table 4 shows the main orbital parameters of four selected constellations, i.e. mainstream GNSS (GPS, Galileo) and LEO mega-constellations (Starlink, OneWeb) that are used for all scenarios of the urban canyon. It is evident that Starlink is a hybrid constellation comprising eight subconstellations of different altitudes and inclinations, while OneWeb has

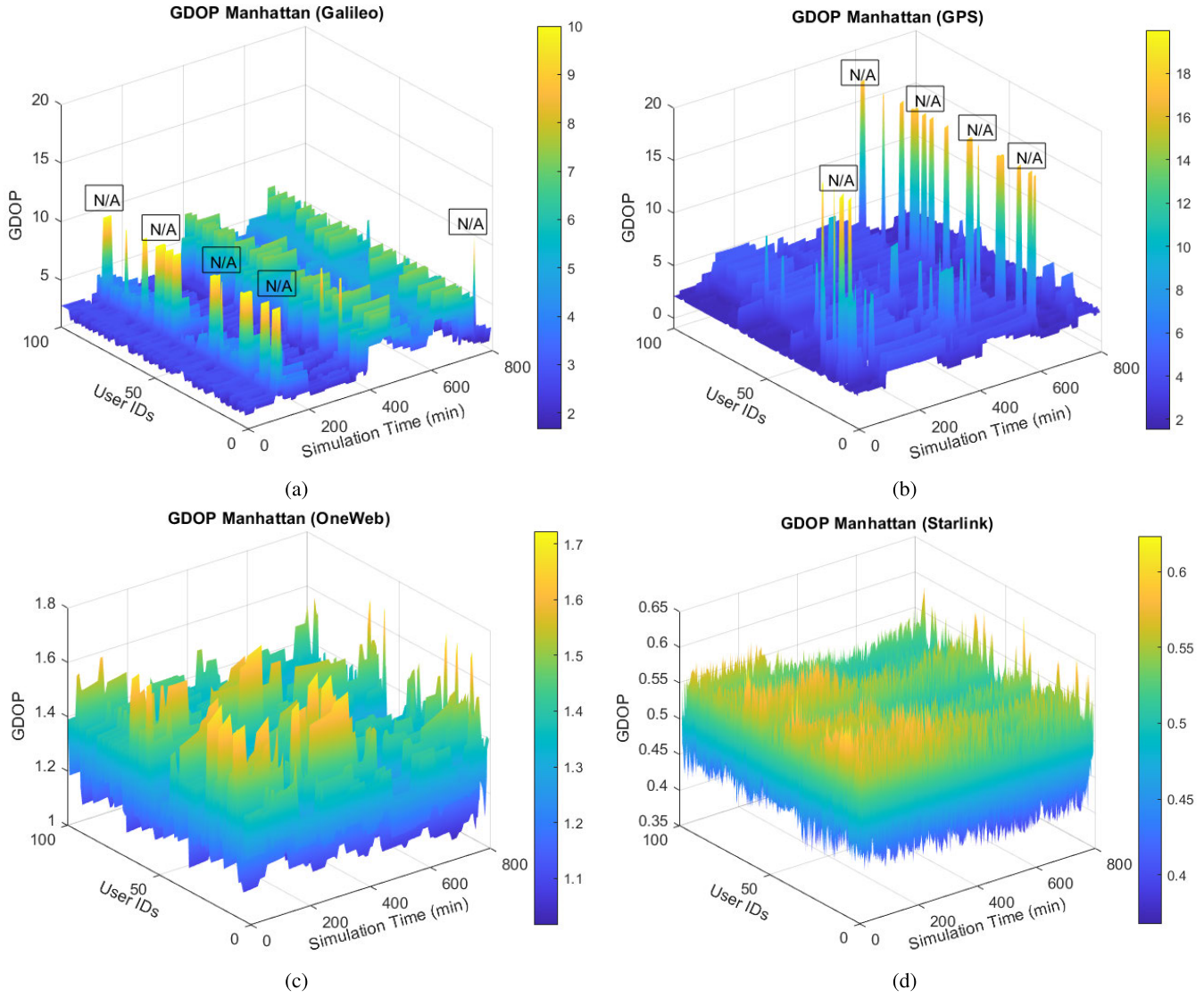

FIGURE 10. GDOP variation for 100 sample user IDs in Manhattan for the constellations: Galileo, GPS, OneWeb, Starlink a simulation time of 800 minutes. In Fig. 10a and Fig. 10b, N/A is the unavailability of a sufficient number of visible satellites for a certain sample user ID at a given epoch. Note the color bars to interpret the scales of the respective graphs.

TABLE 5. GDOP ratings classification [56]. N/A in case of less than 4 visible satellites.

GDOP	Rating
$0 < 1$	Ideal
$1 < 2$	Excellent
$2 < 5$	Good
$5 < 10$	Moderate
N/A	Undefined

polar orbits with an inclination of 87.9°. Furthermore, LEO satellites are approximately two times faster than those in MEO, resulting in a rapid change in the DOP of the LEO mega-constellation. It should be noted that, Table 4 shows the total number of planned satellites in mega-constellations and similar configurations used in the simulation.

The obtained orbital parameters are propagated with a two-body propagator at the epoch of January 1, 2000 [57]. The simulation is developed in Matlab. The simulation period of 800 minutes is chosen considering an approximate complete orbit of the GNSS constellation. During this period, LEO satellites complete several orbits. With the well-known fact that not all satellites within visibility operate simultaneously for Starlink, simulations are conducted under three scenarios: 100%, 70%, and 50% of active satellites randomly selected from the total visible satellites at a specific epoch. Additionally, the ϵ_{min} for the Starlink 70% and 50% active satellites is set to 15°. Therefore, only high-elevation Starlink satellites are used to estimate positioning performance.

Each user, located in London and Manhattan, has a unique urban canyon condition generated statistically using the

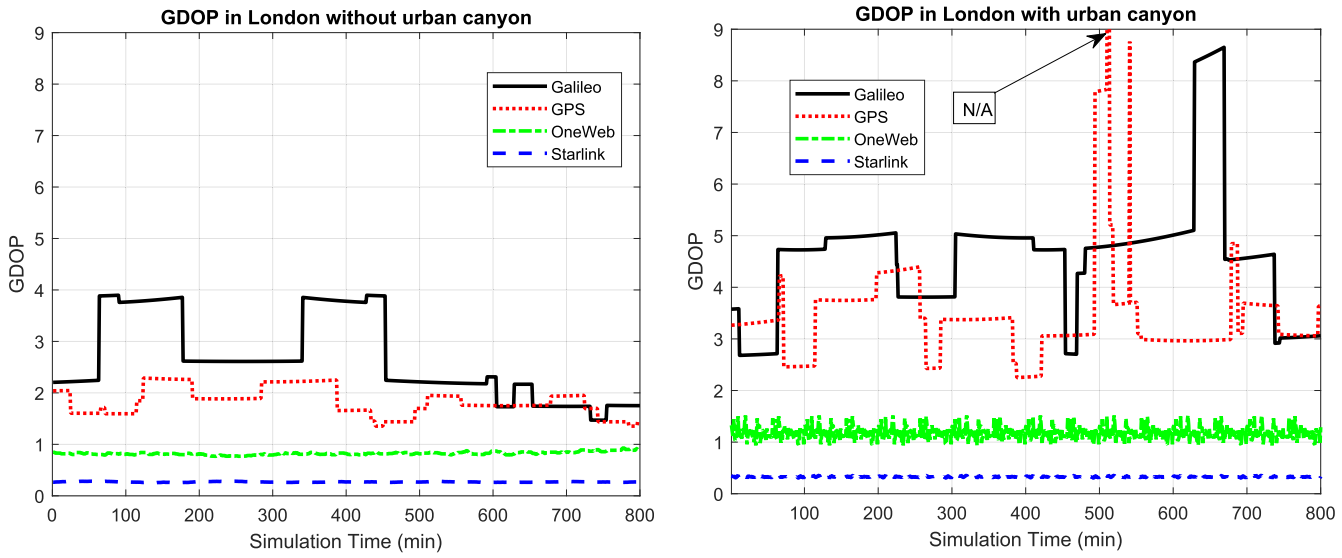

(a) London without urban canyon (b) London with urban canyon

FIGURE 11. GDOP of constellations in London for a sample user ID over a simulation time of 800 minutes.

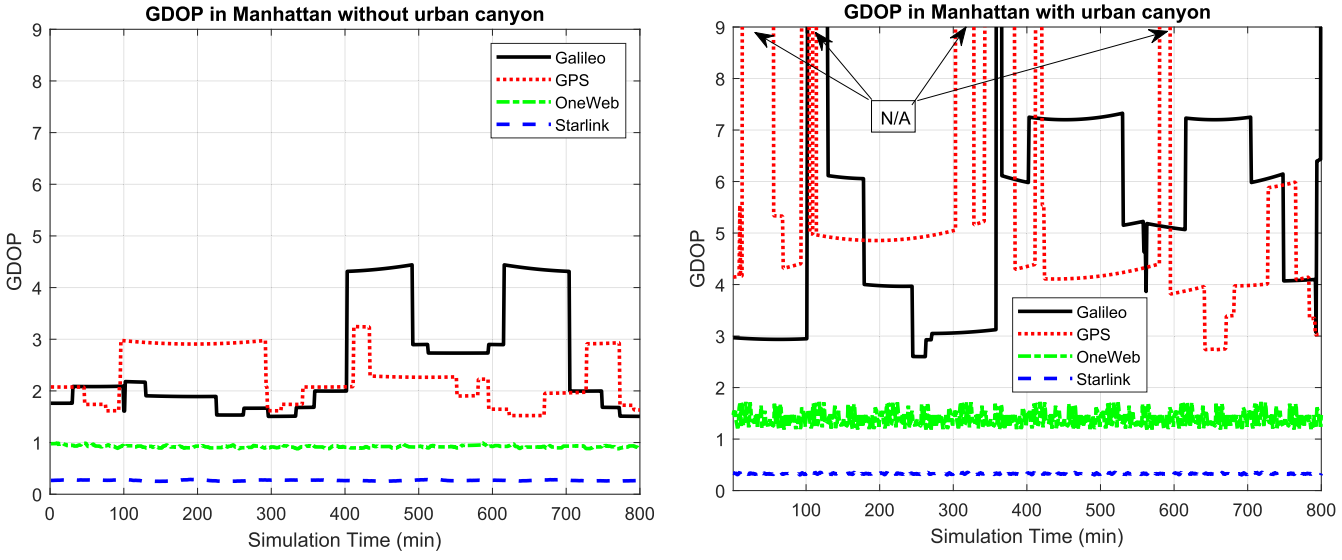

(a) Manhattan without urban canyon (b) Manhattan with urban canyon

FIGURE 12. GDOP of constellations in Manhattan for a sample user ID over a simulation time of 800 minutes.

proposed geometric model and the statistical distribution of the geometric parameters obtained from the available data. 100 different urban canyon dimensions (h, w, d) and rotations (γ) are generated using the respective probability distributions derived in Section III-D. Each generated configuration is called a user ID. For each sample user ID, the satellite visibility and GDOP are estimated.

A statistical analysis of performance in terms of availability and GDOP in London and Manhattan is shown in Sections IV-A and IV-B. Comparative analysis is carried out for the scenarios without and with urban canyons for four selected constellations.

A. PERFORMANCE IN TERMS OF AVAILABILITY

Fig. 6 and Fig. 7 show the number of satellites in visibility for a sample user ID, without and with the urban canyon in London and Manhattan, respectively. The selected user ID is characterized by the following parameters: London ($h = 30$ m, $2d = 12$ m, $w = 40$ m, $\gamma = 0°$) and Manhattan ($h = 60$ m, $2d = 32$ m, $w = 40$ m, $\gamma = 0°$). Moreover, ϵ_{min} of 5° is considered. The dash-dotted curve represents the minimum number of visible satellites necessary for positioning estimation. As expected, the number of satellites in visibility for GPS and Galileo is always close to the minimum value, such as 4 satellites, and sometimes it drops below this

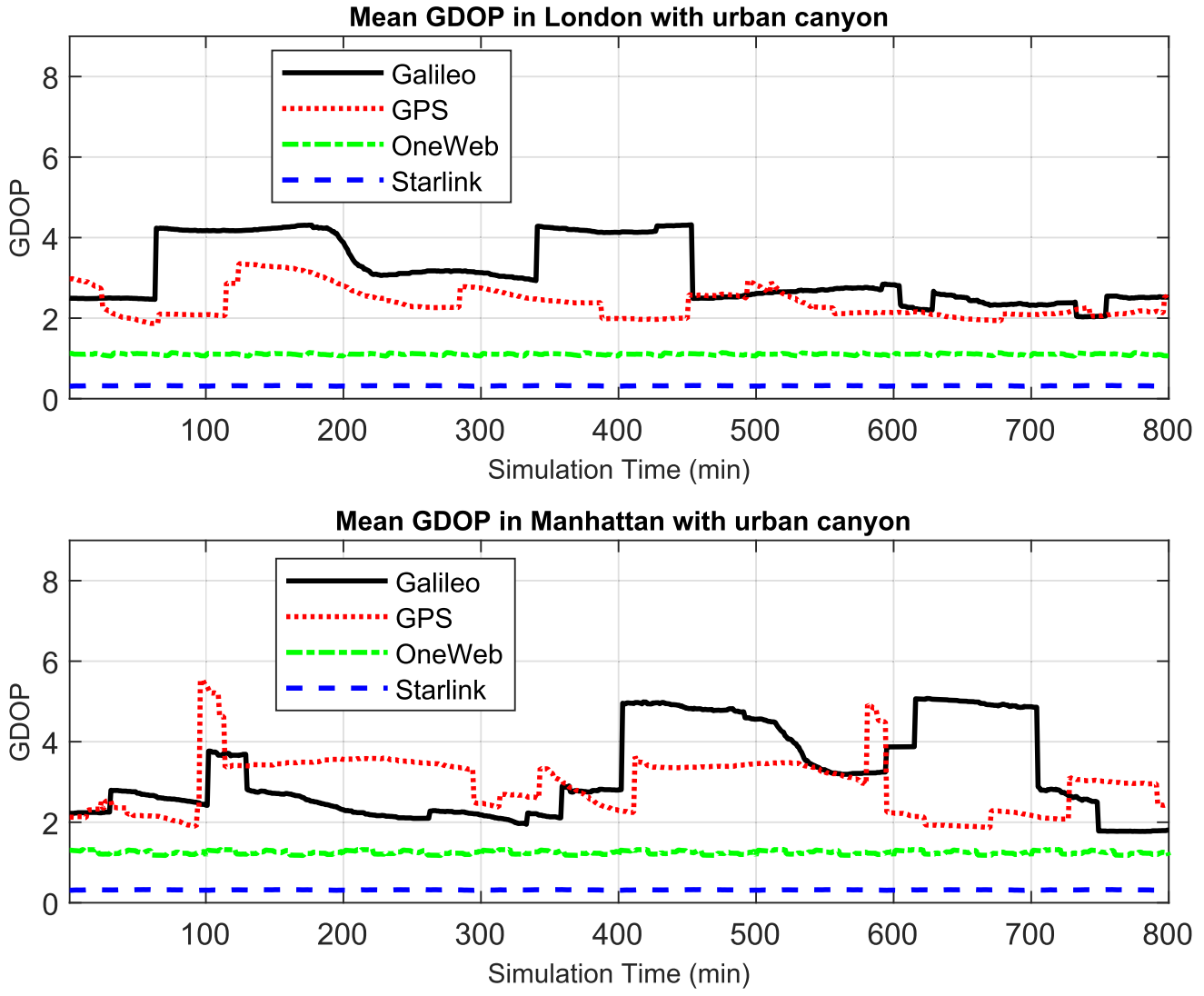

FIGURE 13. Mean GDOP of 100 sample user IDs over a simulation time of 800 minutes with the urban canyon in London and Manhattan.

threshold. On the other hand, the effect of urban canyons on the LEO mega-constellation is negligible. In particular, in the urban canyon scenarios, Starlink consistently has the highest number of visible satellites throughout the simulation period. OneWeb falls in the moderate range, with more than 10 satellites visible at each epoch.

Comparing Fig. 8 of mean satellite visibility with the urban canyon in London and Manhattan reveals that the average satellite visibility in Manhattan is lower than in London due to the presence of deeper urban canyons. In both cities, there are instances where mainstream GNSS fails to provide a sufficient number of visible satellites for a given epoch and a sample user ID. This disparity is not evident in the 2D representations since the curves represent the average values across 100 different sample user IDs.

A statistical summary of the quantitative analysis of availability (%) is presented in Table 6. Interestingly, Starlink shows 100% availability, even with only 70% and 50% active satellites. It is worth highlighting that the average availability of Galileo/GPS and Galileo + GPS, even if it never reaches 100% as in the case of mega-constellations, is rather good, which might be misleading. However, such values are achieved by averaging over the whole possible urban canyon scenarios in the two cities, which are not only characterized by deep urban canyons. Better insights on the benefits of using LEO mega-constellations in big cities characterized by different types of urban canyons can be drawn by the GDOP analysis in the following Section.

B. PERFORMANCE IN TERMS OF GDOP

GDOP analysis is conducted individually for each sample user ID, resulting in 3D plots, while the average GDOP is computed over all the users and over the entire simulation time. In Fig. 9, the 3D graphs illustrate the GDOP variation for different sample user IDs in London. Figures show

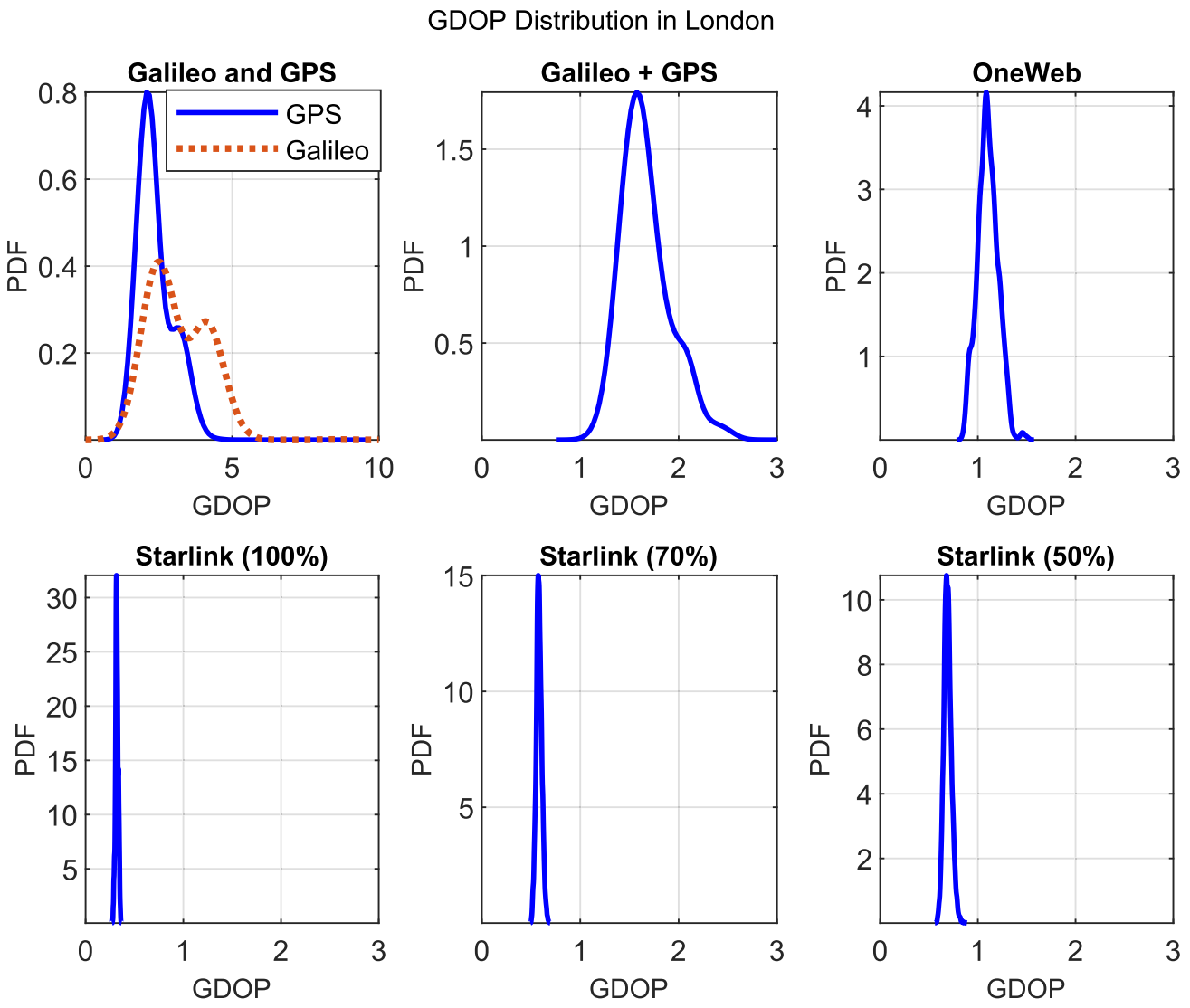

FIGURE 14. GDOP PDF in London for the constellations: Galileo, GPS, Galileo + GPS, OneWeb, Starlink with 100%, 70%, 50% active satellites.

that for a particular user situated in a canyon, the GDOP values exceed 6 for mainstream GNSS and in some instances, service is N/A, as depicted in Fig. 9a and 9b. Conversely, the canyon effect appears to be negligible for LEO mega-constellations, as shown in Fig. 9c and 9d. In the case of OneWeb, the GDOP peaks remain below 1.5, i.e. within the excellent range. On the other hand, Starlink exhibits ideal performance, with the maximum GDOP peak not exceeding 0.45. It is essential to note the color bars to interpret the scales of the respective graphs.

Considering the deep urban canyon, specifically in Manhattan, the GDOP performance is significantly impacted for all four constellations, as depicted in the 3D Fig. 10. For Galileo and GPS, the GDOP peaks reach 20 when the service is N/A as shown in Fig. (10a, Fig. 10b). OneWeb experiences a slight effect due to taller buildings in Manhattan (Fig. 10c) than in London (Fig. 9c), with the maximum GDOP reaching 1.7. In contrast, Starlink consistently operates within the ideal range, with GDOP peaks reaching 0.66, as shown in Fig. 10d.

For a comprehensive comparative analysis to examine the impact of the urban canyon, the GDOP of a sample user ID is plotted against simulation time in Fig. 11 and Fig. 12. The GDOP performance in both cities exhibits an inverse relationship with visibility (Fig. 6 and Fig. 7); high GDOP values correspond to low visibility. Fig. 11a and Fig. 12a focus on GPS and Galileo systems without the presence of an urban canyon. The urban canyon affects all four constellations, as shown in Fig. 11a Vs Fig. 11b and Fig. 12a Vs Fig. 12b. As anticipated, the LEO mega-constellations remain within the excellent and ideal range, while GNSS transitions from the excellent to the moderate range with some instances of service N/A within the deep urban canyon.

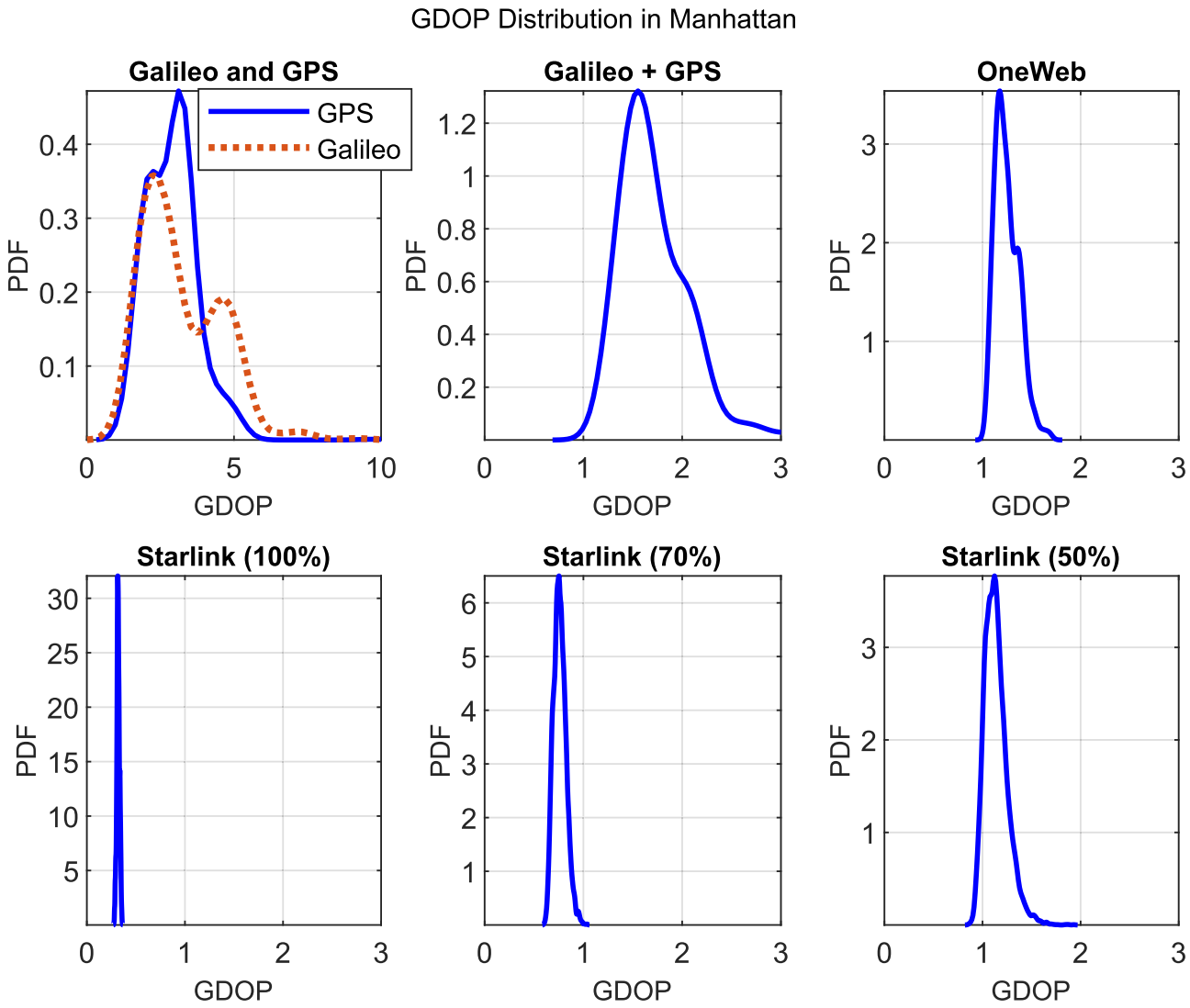

FIGURE 15. GDOP PDF in Manhattan for the constellations: Galileo, GPS, Galileo + GPS, OneWeb, Starlink with 100%, 70%, 50% active satellites.

Fig. 13 presents the plotted average GDOP for all 100 sample user IDs over simulation time in London and Manhattan. Starlink continues to exhibit optimal performance due to its ability to maximize the number of visible satellites at any given epoch. On the other hand, OneWeb demonstrates an average GDOP of approximately 1.25. Due to the canyon effect, the average GDOP values for Galileo and GPS exceed 3. As expected, in Manhattan the average GDOP is worse than in London.

Furthermore, to enhance the statistical interpretation, GDOP distribution (PDF) of Galileo, GPS, Galileo + GPS, OneWeb, and Starlink with 100%, 70%, and 50% active satellites in London and Manhattan is shown in Fig. 14 and Fig. 15 respectively. The PDF is estimated using KDE. Fig. 14 shows the GDOP PDF for the city of London. It can be seen that the GDOP PDF of Starlink is very peaky around the ideal values of GDOP (less than 1) even when 70% or 50% of the visible satellites are considered. This is not the case for GPS or Galileo standalone. In particular, for Galileo, there is no negligible probability that the GDOP is higher than 5. A better distribution of GDOP is achieved by the combination of GPS+Galileo, but in this case, the range is much higher than in the case of mega-constellations i.e., from excellent to good. In the case of Manhattan as shown in Fig. 15, all GDOP PDFs are spread more toward higher values of GDOP, except in the case of Starlink with 100% and 70% active satellites. For 50% satellites in visibility for Starlink, GDOP values reach 1.9, even if the distribution is always in the excellent range similar to OneWeb. In both cities, In the case of OneWeb, the PDF is a little bit more spread, but GDOP stays always in the excellent range. In this way, the GDOP distribution analysis provides a more nuanced perspective on the GDOP characteristics in these urban environments.

Finally, a statistical summary for quantitative analysis of the mean (μ_{gdop}) and standard deviation (σ_{gdop}) of GDOP for

TABLE 6. Summary for quantitative analysis of mean (μ_{gdop}) and standard deviation (σ_{gdop}) of GDOP and availability (%) of the constellations: Galileo, GPS, OneWeb, and Starlink with 100%, 70% and, 50% active satellites, without and with urban canyon environment in London and Manhattan. The above values are estimated for 100 user IDs over a simulation period of 800 minutes. μ_{gdop} and σ_{gdop} corresponds to GDOP distribution shown in Fig. 14 and Fig. 15.

Cities	London						Manhattan					
Urban Canyon	Without			With			Without			With		
Constellation / stats	μ_{gdop}	σ_{gdop}	availability	μ_{gdop}	σ_{gdop}	availability	μ_{gdop}	σ_{gdop}	availability	μ_{gdop}	σ_{gdop}	availability
Galileo	2.64	0.80	100%	3.24	0.74	98.4%	2.54	1.04	100%	3.46	1.14	95.6 %
GPS	1.83	0.27	100%	2.46	0.38	98.6%	2.28	0.53	100%	3.70	3.16	95.6 %
Galileo + GPS	1.49	0.56	100%	1.68	0.035	99%	1.47	0.56	100%	1.72	0.086	97.4%
OneWeb	0.82	0.03	100%	1.10	0.02	100%	0.92	0.02	100%	1.25	0.04	100%
Starlink (100%)	0.29	0.006	100%	0.32	0.003	100%	0.28	0.008	100%	0.48	0.003	100%
Starlink (70%)	0.32	0.001	100%	0.58	0.028	100%	0.32	0.001	100%	0.76	0.069	100%
Starlink (50%)	0.35	0.001	100%	0.69	0.039	100%	0.39	0.004	100%	1.14	0.117	100%

different constellations under various urban canyon scenarios is provided the Table 6. For Galileo/GPS, both with and without an urban canyon, the μ_{gdop} values fall within the good/moderate and excellent/good ranges, respectively. In the case of Galileo + GPS, μ_{gdop}, reaches values of 1.68 and 1.72 for both cities with urban canyons. Conversely, Starlink and OneWeb achieve results within the ideal/excellent range. In Manhattan OneWeb and Starlink (50%) show similar μ_{gdop} of 1.25 and 1.14 which is in the range of excellent. Starlink (100% and 70%) remains in an ideal range below 0.8 under all conditions.

V. CONCLUSION

While it is recognized that mega-constellations could provide better performance than mainstream GNSS systems in urban canyon scenarios, so far no work has statistically assessed such performance improvement. This paper presented a new geometrical model of urban canyon scenarios which has been used for statistical performance analysis of the positioning service in terms of GDOP and availability in representative urban areas, namely the city of London and the Manhattan district of New York City. The performed analysis, besides showing the performance improvement achievable by using mega-constellations both in terms of availability and GDOP, also allows us to get more insights into the performance of different mega-constellations. For instance, while Starlink has the best performance in terms of GDOP (less than 1) and 100% availability in both cities, when the more realistic case in which not all satellites in visibility are considered (for instance, when 50% of satellites are considered), the range of GDOP values increases to 1.9 and gets more similar to the one of OneWeb. However, OneWeb showed performance that is less dependent on the characteristics of the urban canyon. Moreover, the combination of GPS+GALILEO gets about 97.4% to 99% availability and GDOP values in excellent to good range most of the time but is always worse than in the case of mega-constellations. The developed model is rather general and can be used to estimate the performance in other cities/urban canyon areas, but it could be also used as a model for the orbit design of LEO/MEO constellations for positioning services.

REFERENCES

[1] E. D. Kaplan and C. Hegarty, *Understanding GPS/GNSS: Principles and Applications*, 2nd ed. New York, NY, USA: Artech House, 2017.
[2] P. Teunissen and O. Montenbruck, *Springer Handbook of Global Navigation Satellite Systems*, 1st ed. Berlin, Germany: Springer, 2017.
[3] D. Gebre-Egziabher and S. Gleason, *GNSS Applications and Methods*. Norwood, MA, USA: Artech House, 2009.
[4] J. Zidan, E. I. Adegoke, E. Kampert, S. A. Birrell, C. R. Ford, and M. D. Higgins, "GNSS vulnerabilities and existing solutions: A review of the literature," *IEEE Access*, vol. 9, pp. 153960–153976, 2021.
[5] J. Zhang, Y. Cai, C. Xue, Z. Xue, and H. Cai, "LEO mega constellations: Review of development, impact, surveillance, and governance," *Space, Sci. Technol.*, vol. 2022, 2022, doi: 10.34133/2022/9865174.
[6] H. Benzerrouk, Q. Nguyen, F. Xiaoxing, A. Amrhar, H. Rasaee, and R. J. Landry, "LEO satellites based Doppler positioning using distributed nonlinear estimation," *IFAC-PapersOnLine*, vol. 52, no. 12, pp. 496–501, 2019.
[7] T. G. Reid, A. M. Neish, T. F. Walter, and P. K. Enge, "Leveraging commercial broadband LEO constellations for navigating," in *Proc. 29th Int. Tech. Meeting Satell. Division Inst. Navigat.*, Portland, OR, USA, Nov. 2016, pp. 2300–2314, doi: 10.33012/2016.14729.
[8] S. Francis, "Perspectives of PNT services supported by mega-constellations," in *Proc. Int. Tech. Symp. Navigat. Timing (ITSNT)*. Toulouse, France: Airbus Defence and Space -Germany, Nov. 2018.
[9] C. Miao, S. Yu, Y. Hu, H. Zhang, X. He, and W. Chen, "Review of methods used to estimate the sky view factor in urban street canyons," *Building Environ.*, vol. 168, Jan. 2020, Art. no. 106497.
[10] H. Hadidianmoghadam and A. B. Kouki, "New modified urban canyon models for satellite signal propagation prediction," *IEEE Access*, vol. 7, pp. 25298–25307, 2019.
[11] B. Wang, W.-J. Zhao, E.-X. Liu, R. X.-K. Gao, W. Zhang, and C. E. Png, "Satellite visibility and geometry analysis for GNSS positioning in an urban environment," in *Proc. 8th Asia–Pacific Conf. Antennas Propag. (APCAP)*, 2019, pp. 458–459.
[12] B. Krach, A. Lehner, and A. Steingass, "Technical note on the implementation of the land mobile satellite channel model—Software usage," Inst. Commun. Navigat., Tech. Rep., p. 25, Nov. 2005.
[13] J. Bradbury, M. Ziebart, P. A. Cross, P. Boulto, and A. Read, "Code multipath modelling in the urban environment using large virtual reality city models: Determining the local environment," *J. Navig.*, vol. 60, no. 1, pp. 95–105, 2007.
[14] T. Suzuki and N. Kubo, "GNSS positioning with multipath simulation using 3D surface model in urban canyon," in *Proc. 25th Int. Tech. Meeting Satell. Division Inst. Navigat.*, 2012, pp. 438–447.
[15] P. D. Groves, "Shadow matching: A new GNSS positioning technique for urban canyons," *J. Navigat.*, vol. 64, no. 3, pp. 417–430, Jul. 2011.
[16] P. D. Groves, Z. Jiang, L. Wang, and M. Ziebart, "Intelligent urban positioning, shadow matching and non-line-of-sight signal detection," in *Proc. 6th ESA Workshop Satell. Navigat. Technol. (Navitec), Eur. Workshop GNSS Signals Signal Process.*, Dec. 2012, pp. 1–8.
[17] L. Wang, P. D. Groves, and M. K. Ziebart, "GNSS shadow matching: Improving urban positioning accuracy using a 3D city model with optimized visibility scoring scheme," *Navigation*, vol. 60, no. 3, pp. 195–207, Sep. 2013.

[18] L. Wang, P. D. Groves, and M. K. Ziebart, "Multi-constellation GNSS performance evaluation for urban canyons using large virtual reality city models," *J. Navigat.*, vol. 65, no. 3, pp. 459–476, Jul. 2012.
[19] G. E. Taylor, J. Li, D. B. Kidner, and J. M. Ware, "Surface modelling for GPS satellite visibility," in *Proc. Int. Workshop Web Wireless Geographical Inf. Syst.*, 2005, pp. 281–295.
[20] G. Taylor, J. Li, D. Kidner, C. Brunsdon, and M. Ware, "Modelling and prediction of GPS availability with digital photogrammetry and LiDAR," *Int. J. Geographical Inf. Sci.*, vol. 21, no. 1, pp. 1–20, Jan. 2007.
[21] Y.-W. Lee, Y. Suh, and R. Shibasaki, "Simulation-based estimation of multipath mitigation using 3D-GIS and spatial statistics," in *Proc. 19th Int. Tech. Meeting Satell. Division The Inst. Navigat.*, 2006, pp. 1778–1783.
[22] H.-F. Ng, L.-T. Hsu, M. J. L. Lee, J. Feng, T. Naeimi, M. Beheshti, and J.-R. Rizzo, "Real-time loosely coupled 3DMA GNSS/Doppler measurements integration using a graph optimization and its performance assessments in urban canyons of new York," *Sensors*, vol. 22, no. 17, p. 6533, Aug. 2022. [Online]. Available: https://www.mdpi.com/1424-8220/22/17/6533
[23] F. Causa and G. Fasano, "Improving navigation in GNSS-challenging environments: Multi-UAS cooperation and generalized dilution of precision," *IEEE Trans. Aerosp. Electron. Syst.*, vol. 57, no. 3, pp. 1462–1479, Jun. 2021.
[24] J. Li, G. Taylor, D. Kidner, and M. Ware, "Prediction of GPS multipath effect using LiDAR digital surface models and building footprints," in *Web and Wireless Geographical Information Systems*. Hong Kong: Springer, 2006, pp. 42–53.
[25] Y. Suh and R. Shibasaki, "Evaluation of satellite-based navigation services in complex urban environments using a three-dimensional GIS," *IEICE Trans. Commun.*, vols. 90, no. 7, pp. 1816–1825, Jul. 2007.
[26] Y.-W. Lee, Y. Suh, and R. Shibasaki, "A GIS-based simulation to predict GPS availability along the Tehran road in Seoul, Korea," *KSCE J. Civil Eng.*, vol. 12, no. 6, pp. 401–408, Nov. 2008.
[27] S. Ji, W. Chen, X. Ding, Y. Chen, C. Zhao, and C. Hu, "Potential benefits of GPS/GLONASS/GALILEO integration in an urban canyon—Hong Kong," *J. Navigat.*, vol. 63, no. 4, pp. 681–693, Oct. 2010.
[28] H. More, M. De Sanctis, E. Cianca, and C. Stallo, "GDOP optimised LEO constellation for positioning estimation," in *Proc. 12th CONASENSE Symp.*, 2022, pp. 1–8.
[29] F. Ma, X. Zhang, X. Li, J. Cheng, F. Guo, J. Hu, and L. Pan, "Hybrid constellation design using a genetic algorithm for a LEO-based navigation augmentation system," *GPS Solutions*, vol. 24, no. 2, pp. 1–14, Apr. 2020.
[30] F. Dufouf, R. Bertrand, J. Sarda, E. Lasserre, and J. Bernussou, "Constellation design optimization with a DOP based criterion," in *Proc. 14th Int. Symp. Space Flight Dyn.*, 1999, pp. 1–8.
[31] XONA. (2023). *LEO Pnt Xona Space System*. [Online]. Available: https://www.xonaspace.com/
[32] L. Wang, R. Chen, B. Xu, X. Zhang, T. Li, and C. Wu, "The challenges of LEO based navigation augmentation system—Lessons learned from Luojia-1A satellite," in *Proc. China Satellite Navigat. Conf.*, J. Sun, C. Yang, and Y. Yang, Eds. Singapore: Springer, 2019, pp. 298–310.
[33] G-World. (2020). *Egnos Payload Enters Service on Eutelsat 5 West B*. [Online]. Available: https://www.gpsworld.com/egnos-payload-enters-service-on-eutelsat-5-west-b/
[34] P. A. Iannucci and T. E. Humphreys, "Economical fused LEO GNSS," in *Proc. IEEE/ION Position, Location Navigation Symp. (PLANS)*, 2020, pp. 426–443.
[35] Z. Kassas, J. Morales, and J. Khalife, "New-age satellite-based navigation—STAN: Simultaneous tracking and navigation with LEO satellite signals," *Inside GNSS Mag.*, vol. 14, pp. 56–65, Apr. 2019.
[36] R. Morales-Ferre, E. S. Lohan, G. Falco, and E. Falletti, "GDOP-based analysis of suitability of LEO constellations for future satellite-based positioning," in *Proc. IEEE Int. Conf. Wireless Space Extreme Environments (WiSEE)*, Oct. 2020, pp. 147–152.
[37] T. G. R. Reid, A. M. Neish, T. Walter, and P. K. Enge, "Broadband LEO constellations for navigation," *Navigation*, vol. 65, no. 2, pp. 205–220, Jun. 2018.
[38] NORAD. (2023). *Two-Line-Element*. [Online]. Available: https://www.celestrak.org/
[39] G. Xiao-Zhong, L. Jia-Wei, S. Ming, G. Peng-Qi, Y. Da-Tao, Y. Huan-Huan, and Z. You, "Analysis on propagation accuracy of deep-space TLE objects affected by solar/lunar orbit calculation," *Chin. Astron. Astrophys.*, vol. 47, no. 1, pp. 221–235, Jan. 2023. [Online]. Available: https://www.sciencedirect.com/science/article/pii/S0275106223000012
[40] A. Bourdeau, M. Sahmoudi, and J.-Y. Tourneret, "Tight integration of GNSS and a 3D city model for robust positioning in urban canyons," in *Proc. 25th Int. Tech. Meeting Satell. Division Inst. Navigat.*, vol. 2, 2012, pp. 1263–1269.
[41] R. M. Alkan, V. Ilçi, I. M. Ozulu, and M. H. Saka, "A comparative study for accuracy assessment of PPP technique using GPS and GLONASS in urban areas," *Measurement*, vol. 69, pp. 1–8, Jun. 2015. [Online]. Available: https://www.sciencedirect.com/science/article/pii/S0263224115001542
[42] N. Nadarajah, P. J. G. Teunissen, and N. Raziq, "Instantaneous GPS-Galileo attitude determination: single-frequency performance in satellite-deprived environments," *IEEE Trans. Veh. Technol.*, vol. 62, no. 7, pp. 2963–2976, Sep. 2013.
[43] H. Xu and L.-T. Hsu, "Urban buildings update monitoring based on sky visibility estimation using GNSS and LEO," *J. Navigat.*, pp. 1775–1783, Sep. 2022.
[44] D. Racelis, B. Pervan, and M. Joerger, "Fault-free integrity analysis of mega-constellation-augmented GNSS," in *Proc. 32nd Int. Tech. Meeting Satell. Division Inst. Navigat.*, Oct. 2019, pp. 465–484.
[45] J. S. Subirana, J. M. J. Zornoza, and M. Hernández-Pajares, "Transformations between ECEF and ENU coordinates," Univ. Catalonia, Spain, Tech. Rep., 2011.
[46] L. Wang, P. D. Groves, and M. K. Ziebart, "Smartphone shadow matching for better cross-street GNSS positioning in urban environments," *J. Navigat.*, vol. 68, no. 3, pp. 411–433, 2015.
[47] G. R. Terrell and D. W. Scott, "Variable kernel density estimation," *Ann. Statist.*, vol. 20, no. 3, pp. 1236–1265, Sep. 1992. [Online]. Available: http://www.jstor.org/stable/2242011
[48] D. W. Scott, *Multivariate Density Estimation: Theory, Practice, and Visualization*. Hoboken, NJ, USA: Wiley, 2015.
[49] MATLAB. (2022). *Curve Fitting Tool Box MATLAB*. [Online]. Available: https://it.mathworks.com/help/curvefit/curvefitter-app.html#butc97o-1
[50] D. Joyce. (2014). *Common Probability Distributionsi*. Math 217 Probability and Statistics. [Online]. Available: http://aleph0.clarku.edu/ djoyce/ma217/distributions.pdf
[51] EMU. Analytics. *London—Buildings Database*. Accessed: Oct. 4, 2022. [Online]. Available: https://www.emu-analytics.com/products/datapacks
[52] Kaggle. *New York City—Buildings Database*. Accessed: 2017. [Online]. Available: https://www.kaggle.com/datasets/new-york-city/nyc-buildings
[53] OpenStreetMap Contributors. (2017). *Planet Dump Retrieved*. [Online]. Available: https://planet.osm.org
[54] X. Li, F. Ma, X. Li, H. Lv, L. Bian, Z. Jiang, and X. Zhang, "LEO constellation-augmented multi-GNSS for rapid PPP convergence," *J. Geodesy*, vol. 93, no. 5, pp. 749–764, May 2019.
[55] L. Salvadori, A. Di Bernardino, G. Querzoli, and S. Ferrari, "A novel automatic method for the urban canyon parametrization needed by turbulence numerical simulations for wind energy potential assessment," *Energies*, vol. 14, no. 16, p. 4969, Aug. 2021. [Online]. Available: https://www.mdpi.com/1996-1073/14/16/4969
[56] O. K. Isik, J. Hong, I. Petrunin, and A. Tsourdos, "Integrity analysis for GPS-based navigation of UAVs in urban environment," *Robotics*, vol. 9, no. 3, p. 66, Aug. 2020.
[57] W. D. Vallado and D. A. McClain, *Fundamentals of Astrodynamics and Applications*. New York, NY, USA: McGraw-Hill, 1997.

HARSHAL MORE received the B.Tech. degree in aerospace engineering from IGNOU, New Delhi, India, and the M.Sc. degree in space and astronautical engineering from the Sapienza University of Rome, Rome, Italy, in 2021. He is currently pursuing the Ph.D. degree with the Department of Electronics Engineering, University of Rome "Tor Vergata," Italy. He received an II Level Master in engineering and International Space Law in satellite systems for communication, navigation, and sensing with high honors. His research interests include GNSS, LEO PNT, space mission analysis, and space robotics. He received the Best Paper Award from the 2022 International Symposium on Wireless Personal Multimedia Communications (WPMC 2022).

ERNESTINA CIANCA (Member, IEEE) was employed by Aalborg University, Denmark, as a Research Engineer, from 2000 to 2001, and an Assistant Professor with the Wireless Networking Group (WING), from 2001 to 2003. She was an Assistant Professor with the University of Rome ''Tor Vergata,'' from 2003 to 2019. She is currently an Associate Professor with the Department of Electronics Engineering, University of Rome ''Tor Vergata,'' where she teaches: the Internet of Things-principles and applications; digital communications; and internet delle cose. She is the Director of the Master Program in Engineering and International Space Law in Communication, Navigation, and Sensing via Satellite. She is the Vice-Director of the Interdepartmental Research Center, Center for TeleInFrastructures (CTIF), University of Rome ''Tor Vergata.'' She is the author of more than 150 papers published in international journals and conference proceedings. She has participated in several European and national projects. She has been responsible for the University of Rome ''Tor Vergata'' activities in the several Italian Space Agency and ESA Projects.

MAURO DE SANCTIS received the Ph.D. degree in telecommunications and microelectronics engineering from the University of Rome ''Tor Vergata,'' Italy, in 2006.

From January 2004 to December 2005, he was involved in the *My Personal Adaptive Global NET* (MAGNET) European FP6 Integrated Project and the SatNEx European Network of Excellence. In 2006, he was a Postdoctoral Research Fellow with the European Space Agency (ESA) ARIADNA extended study named ''The Flower Constellation Set and its Possible Applications.'' From January 2006 to June 2008, he was involved in the MAGNET Beyond European FP6 Integrated Project as scientific responsible for the WP on Coexistence of Radio Interfaces. He was with the Italian Space Agency (ASI) as a Holder of a two-year research scholarship on the study of Q/V band satellite communication links for a technology demonstration payload, which concluded, in 2008, during this period he participated in the opening and the first trials of the ASI Concurrent Engineering Facility (ASI-CEF). Since 2008, he has been an Assistant Professor with the Department of Electronics Engineering, University of Rome ''Tor Vergata.'' In 2009, he was involved in the ESA Project on Multipurpose Constellation. From 2010 to 2011, he was involved in the ESA Project Telemedicine Services for Health (TESHEALTH). He is currently an Associate Professor of telecommunications with the Department of Electronics Engineering, University of Rome ''Tor Vergata,'' teaching information theory and data science. He is a Founder Member with the University Spin-Off RadioPoints s.r.l. He published more than 130 papers in journals and conference proceedings, seven book chapters, one book, and one patent. His main research interests include wireless terrestrial and satellite communication networks, wireless localization and sensing, data science, and information theory.

Dr. De Sanctis was a co-recipient of the Best Paper Awards from the 2009 International Conference on Advances in Satellite and Space Communications (SPACOMM 2009) and the 2022 International Symposium on Wireless Personal Multimedia Communications (WPMC 2022). He is serving as an Associate Editor for the Command, Control, and Communications Systems Area of IEEE TRANSACTIONS ON AEROSPACE AND ELECTRONIC SYSTEMS and the Signal Processing and Communication Area of *IEEE Aerospace and Electronic Systems Magazine*.

Open Access funding provided by 'Università degli Studi di Roma "Tor Vergata"' within the CRUI CARE Agreement